IECON 2022 – 48th Annual Conference of the IEEE Industrial Electronics Society | 978-1-6654-8025-3/22/$31.00 ©2022 IEEE | DOI: 10.1109/IECON49645.2022.9969110

A Supercapacitor and Fuzzy-PID Controller-based Active Charge Balancing Scheme for Lithium-ion Batteries

Akash Samanta (*Student Member, IEEE*)
Department of Electrical, Computer and Software Engineering
Ontario Tech University
Oshawa, Canada
akash.samanta@ontariotechu.net

Mohit Sharma
Weld Aid Automation
Kolkata, India
mohitsharma@weldaidautomation.com

Sheldon Williamson (*Fellow, IEEE*)
Department of Electrical, Computer and Software Engineering
Ontario Tech University
Oshawa, Canada
Sheldon.Williamson@ontariotechu.ca

***Abstract*—A hybrid Fuzzy proportional-integral-derivative (Fuzzy-PID)-based control algorithm is introduced for a non-dissipative (active) charge equalization scheme consisting of a supercapacitor and two-stage bidirectional DC-DC converter. The proposed control algorithm intelligently modulates the balancing parameters while realizing the cell-to-pack-to-cell (C2P2C) balancing of a lithium-ion battery pack. The charge imbalance and charging/discharging profile are considered by the Fuzzy-logic algorithm to determine the balancing current that not only enhances the balancing speed but also ensures the operation under a safe operating region and a longer battery life. Accurate determination of cell state of charge (SOC) is highly challenging, here the proposed Fuzzy-based control algorithm eliminates the necessity of accurate SOC determination that eventually reduces the computational cost and necessity of highly precise sensors. The proposed topology requires fewer active components due to the utilization of C2P2C balancing, resulting in a simple control algorithm and lower implementation cost. The supercapacitor is used as an energy buffer to enhance the robustness and life of the balancing circuitry. Simulation studies are conducted in MATLAB-Simscape to verify the effectiveness of the proposed scheme. Further, a comparative study with the state-of-the-art is performed to demonstrate the superiority of the scheme.**

Keywords— equalization, electric vehicle, energy storage, artificial intelligence, intelligent control

I. INTRODUCTION

There is a causal relationship between cell balancing, optimum capacity utilization, and safety of a lithium-ion battery (LIB) pack. Numbers of LIB cells are connected in series to obtain the desired voltage. Due to the unavoidable manufacturing inconsistency, uneven battery aging, and operating temperature the cell voltage and stored charge become imbalanced over time. Prolonged operation of the battery pack without a proper cell balancing scheme leads to escalated aging and safety issues and even catastrophic failure. A proper cell balancing scheme also ensures optimum capacity utilization and longer operational life. Broadly, the cell balancing scheme can be grouped based on the utilization of balancing energy. The passive balancing scheme uses simple resistor-based circuits to dissipate the excess energy from the highest charged cell, in contrast, the active balancing scheme transfers the excess energy to low-energy cells or the entire battery pack through an energy buffer circuit without dissipating energy. Commonly, capacitors, inductors, transformers, and DC-DC converters are used as the energy buffer circuit. Further, active balancing schemes can also be grouped based on the balancing energy transfer path such as pack to cell (P2C) [1], cell to pack (C2P) [2], direct cell to cell (DC2C) [3], adjacent cell to cell (AC2C) [4], any cell to any cell (AC2AC) [5], and multicell-to-multicell-to-multicell (MC2MC) [6] methods. Among these C2P balancing during the charging period and P2C balancing during discharging period provides an optimum balancing path, faster balancing, and reduced requirement of active power electronics components [7].

Previously, Sani et al. [8] proposed a switched capacitor scheme where two cells are used to charge the buffer capacitor instead of a single cell which helps minimizes the low voltage difference between cells and capacitor resulting in improved balancing speed. A downside is if one cell of the pair has a lower SOC than the average SOC of the pack, then the method will further discharge the cell instead of charging. This condition may lead to further imbalances instead of balancing. Friansa et al. [9] used an auxiliary battery capacitor and a DC-DC boost converter to boost the voltage while transferring energy to the lowest cell. The use of an auxiliary unit and maintaining enough charge before balancing are the prime limitations. Baronti et al. [10] proposed a supercapacitor and DC-DC converter-based DC2C balancing scheme but the control strategy used is very complex and outdated such as using a significant number of PMOSFETs slowing balancing speed. Jiang et al. [11] proposed a single supercapacitor and cell bypassing-based balancing scheme. However, online bypassing of cells carrying a very high discharge current is impractical and risky. Moreover, the balancing speed and efficiency are very low as balancing can only be possible during the regeneration period.

Therefore, it can be noted that high balancing time, efficiency, implementation cost, and control complexity are the major concerns in cell balancing schemes. Therefore, in this paper a cell-to-pack-to-cell (C2P2C) balancing scheme is proposed where a supercapacitor is used as an energy buffer and a buck-boost converter is used to control the balancing voltage. Further, the conventional average cell voltage/ SOC-based control algorithms do not modulate the balancing current based on the voltage/SOC difference and do not consider the charging/discharging profile. These lead to early failure and safety issues. Therefore, the Fuzzy-PID-based [12] cell balancing control scheme is introduced to modulate the

balancing current based on the SOC and voltage difference, and the SOC status of the battery during charging/discharging.

II. BALANCING CIRCUIT AND DYNAMIC

A. Circuit Topology

Fig. 1 depicts the circuit topology of the proposed supercapacitor and bidirectional DC-DC converter and Fuzzy-PID controller-based active cell balancing scheme.

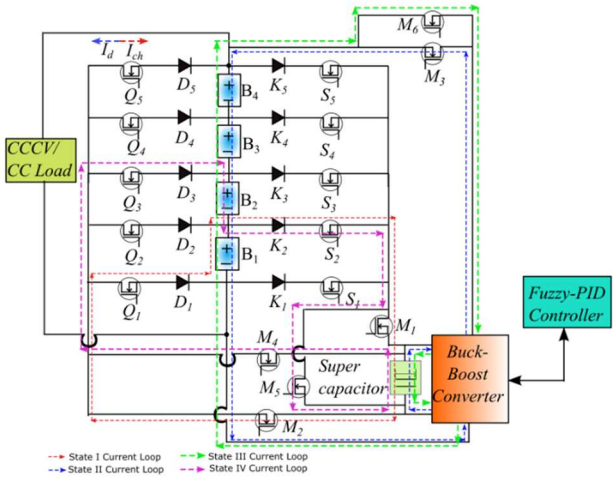

Fig. 1. Proposed active balancing scheme with the energy flow direction.

B. Working Principle

For ease of understanding, the proposed balancing scheme is implemented for a 4S-1P LIB pack (four series-connected cells in a single string) as shown in Fig.1 where B_1,...,B_4 represent the serially connected cells. The cell selection network consists of Q_1-Q_{4+1} and S_1-S_{4+1} power switches along with D_1-D_{4+1} and K_1-K_{4+1} power diode. Diodes are used to restrict the power flow directions. The DC-DC converter, supercapacitor, and fixed number of power switches (M_1 to M_6) are used in the balancing power transfer network. The Fuzzy-PID controller modulates the balancing parameters depending on the SOC difference (ΔSOC), cell voltage difference (ΔV), and SOC_{avg} in real-time. A constant current constant voltage (CCCV) charging protocol and a constant current load is considered for this study.

During the charging period, the algorithm (Fig. 2) first determines the cell with maximum SOC and the cell with minimum SOC. Then the power transfer network transfers the excess charge from the highest SOC cell to the lowest SOC cell with the help of a supercapacitor and DC-DC converter. During this process, the excess energy is first stored in the supercapacitor (state I) and then in the next cycle the supercapacitor is discharged, and the power is transferred to the battery pack (state II). Collectively, the state I and state II realize the C2P balancing during the charging period. In contrast, during the discharging period, at first, the supercapacitor is charged from the battery pack in the first part of the balancing cycle (state III), and then the energy is transferred to the lowest SOC cell (state IV) through the DC-DC converter. In this mode, the P2C balancing operation is realized. The switching frequency between the states is considered as *f=1 Hz*. The duty ratio is dynamically determined by the Fuzzy-PID controller to control the balancing current depending on the battery parameters. As an example, at a particular time instant t, if B_1 is the most charged cell during the charging period and B_2 is the least charged cell during the discharging period, then the direction of current flow and active switches in each of these four states are shown in Fig.1.

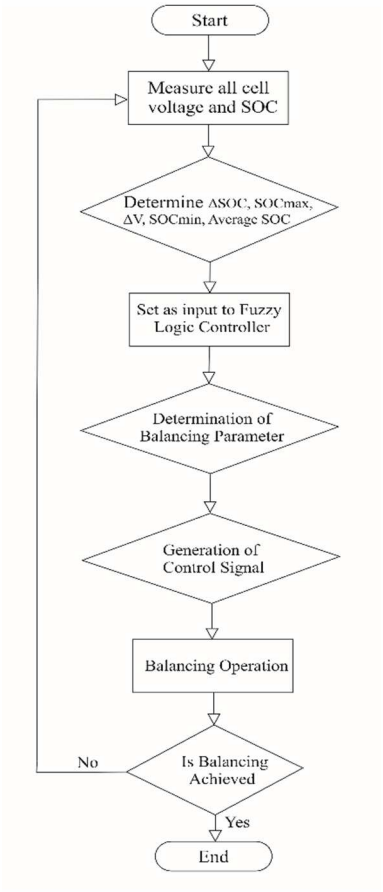

Fig.2. Flow chart of the balancing algorithm.

C. Dynamics of the balancing Topology

The terminal voltage of the supercapacitor is almost linear to its stored charge as shown in Fig. 3 which makes them ideal for the energy buffer circuit of the cell balancing network [13]. The characteristics can be mathematically represented as (1).

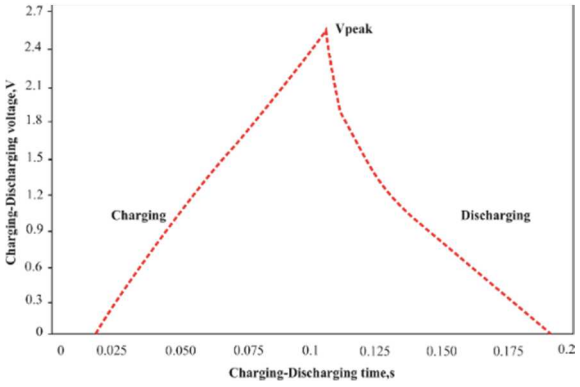

Fig 3. Charging and discharging behavior of supercapacitor.

$$\frac{V_t}{V_{int}} = \frac{Q_t}{Q_{int}} \frac{C_n}{C_n} \quad (1)$$

$I_{sc,c}$ = SC charge current
$V_{sc,c}$= SC charge voltage
t_0 = initial condition time
τ = time constant
$I_{sc,d}$ = SC discharge current
V_{cd} = SC discharge voltage
V_{Pack}= Stack voltage
Ƞ = efficiency
$\Delta V = V_{sc,d} - V_{pack}$
C_n = Capacitance of SC
Q_t = Stored charged in SC at t
Q_{int} =Initial stored charged in SC
V_t = Voltage across SC at t
V_{int} = Initial voltage across SC

Here, Q_t and Q_{int} are the storage charge of supercapacitor at time instant t and the initial condition respectively. Similarly, V_t and V_{int} are the voltage across the capacitor when the stored charge is Q_t and Q_{int} respectively.

Further, the charging and discharging voltage and current of the supercapacitor can be calculated using (2) to (5). All power switches are ideal for ease of understanding and calculation.

$$I_{sc,c} = -\frac{(V_{sc}(t_0)-V_{batt})}{R_{cell}} e^{-(t_1-t_0)/\tau} \quad (2)$$

$$V_{sc,c} = V_{sc}(t_1) + (V_{sc}(t_0) - V_b)\left(1 - e^{-(t_1-t_0)/\tau}\right) \quad (3)$$

$$I_{sc,d} = \frac{\left(\frac{D}{1-D}V_{sc}(t_2)-V_{Pack}\right)}{R_{series}} e^{-(t_2-t_1)/\tau} \quad (4)$$

$$V_{cd} = V_{Pack} + \left(\frac{D}{1-D}V_{sc}(t_2) - V_{Pack}\right) e^{-(t_2-t_1)/\tau} \quad (5)$$

Now the amount of energy transfer in a balancing cycle and the efficiency can be calculated using (6) and (7).

$$E = \int v_{discharge} * i_{discharge} dt = C\Delta V \left(\frac{\Delta V}{2} e^{-\frac{t}{\tau}} - V_{pack} * e^{-\frac{t}{\tau}}\right) - \left[\frac{\Delta V}{2} - V_{pack}\right] \quad (6)$$

$$\eta = \frac{E_{Transfred}}{E_{Initial}} = \frac{\sum_{k=1}^{n}|E_{n,LV\ After} - E_{n,LV\ Before}|}{\sum_{k=1}^{n}|E_{n,HV\ Before} - E_{n,HV\ After}|} x100 \quad (7)$$

III. DESIGN OF FUZZY-PID BALANCING CONTROLLER

A. Block Diagram of the Controller

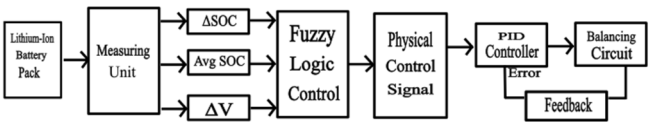

Fig 4. Block diagram of Fuzzy-PID control algorithm.

At first, the fuzzy controller considers the value of ΔSOC, SOC_{avg}, ΔV as the input signal from the battery pack as shown in Fig. 4. Then, the Fuzzy logic controller process the input data in three sequential stages namely, fuzzification, inference, and defuzzification. Finally, the physical control signal is generated and sent to the PID controller. The PID controller then ensures the proper level of balancing current set by the Fuzzy controller considering the feedback of the present balancing current.

B. Generation of Control Signals from Fuzzy Controler

The Fuzzy inference system consists of a Fuzzy rule base that is defined using different membership functions. The block diagram of the fuzzy-based control system is shown in Fig. 5. The membership function used for three input variables (ΔV and ΔSOC, and SOC_{avg}) in the Fuzzy system is shown in Fig. 6.

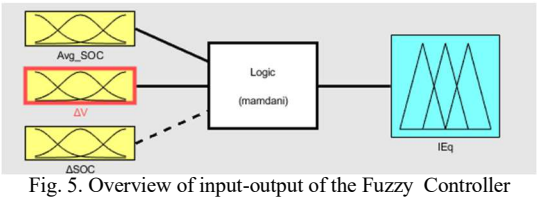

Fig. 5. Overview of input-output of the Fuzzy Controller

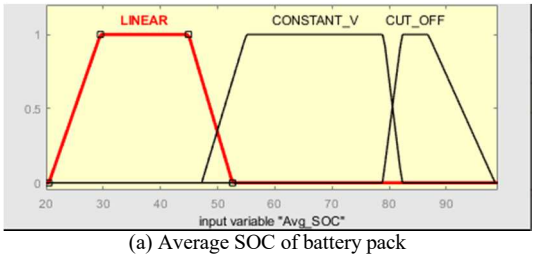

(a) Average SOC of battery pack

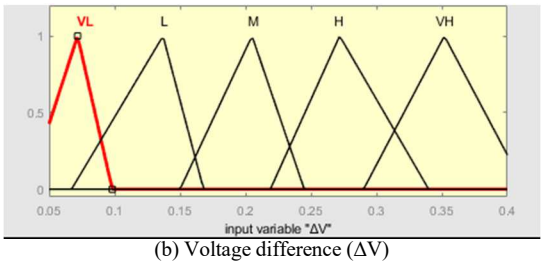

(b) Voltage difference (ΔV)

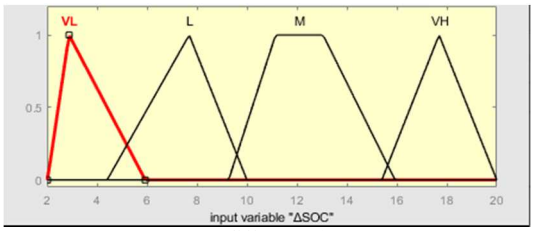

(c) SOC difference (ΔSOC)

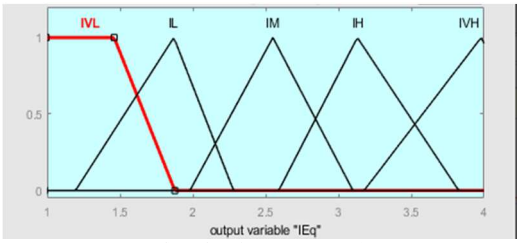

(d) Balancing current (I_{eq})

Fig. 6. Fuzzy membership function (a) SOC_{avg} of battery pack, (b) Voltage difference (ΔV), (c) SOC difference (ΔSOC), (d) Balancing current (I_{eq}).

Fig. 7 described how the Fuzzy control system generates the equivalent balancing current (I_{eq}) with different combinations of input battery parameters including ΔV and ΔSOC, and SOC_{avg}. Here, in this case, the membership function is defined in three different regions to capture the charging/discharging characteristics of the LIB cell. The charging/discharging characteristics of LIB is divided into three regions namely, linear region (SOC_{avg} = 20% to 50%), constant voltage region (SOC_{avg} =50% to 80%), and cut-off region (SOC_{avg} =80%-100%). In the first region, the voltage and SOC rise linearly, however, in the constant voltage region the change in voltage is negligible but the SOC changes very rapidly.

Whereas, in the range between 80% - 100% again almost linear changes in SOC and voltage can be noticed. Presently none of the balancing methods modulates the balancing current based on the SOC status of a battery pack charging/discharging. Providing a high balancing current at the end of cell charging leads to early aging. In contrast, providing a low balancing current at the beginning of charging leads to slow balancing.

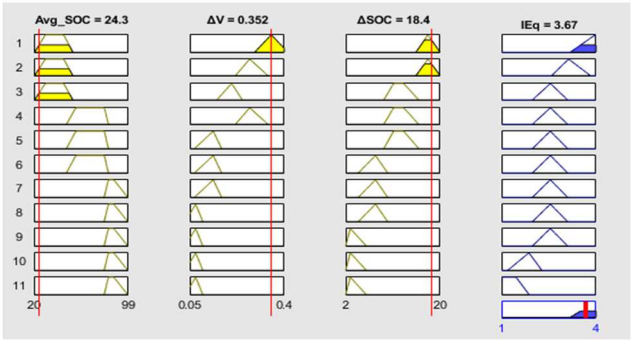

(a) Balancing current at ΔV = 0.352 V & ΔSOC = 18.4%

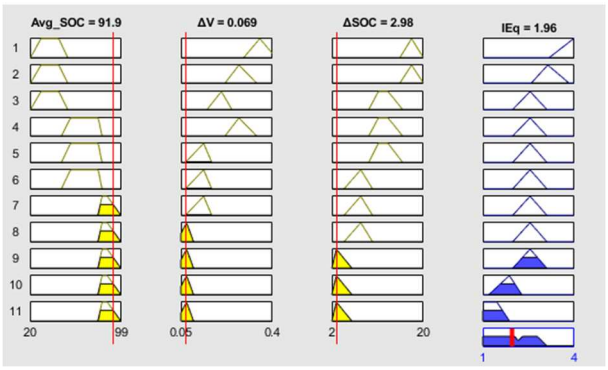

(b) Balancing current at ΔV = 0.069 V & ΔSOC = 2.98%

Fig. 7. Balancing current at different combinations of battery parameters

The modulation of balancing current by the Fuzzy-controller at different combinations of battery parameters is shown in Fig. 8. Finally, five linguistic variables namely, VH (very high), H (high), M (medium), L (low), and VL (very low) using a combination of triangular and trapezoidal forms are used for describing the membership function in the Fuzzy inference system. The three-dimensional (5 X 5 X 3) rule matrix for the linguistic variables is shown in Table I.

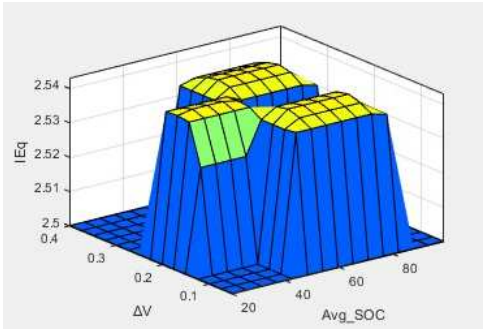

Fig. 8. Switching surface of the Fuzzy logic output corresponding to the input.

TABLE I. DESIGN RULES OF FUZZY LOGIC CONTROLLER

Input variable						
ΔV	$\overline{SOC}$	ΔSOC				
VL	Linear region	VL	L	M	H	VH
		VL	L	M	H	VH
L	Constant Voltage region	L	L	L	VH	VH
M		L	L	M	M	M
H	Cutoff region	L	L	VL	VL	VL
VH		L	L	VL	VL	VL

C. Fuzzy PID Control Strategy

In this work, Fuzzy-PID controller with type-2 Sugeno fuzzy inference systems is adapted from [14]. The controller structure as described in Fig. 4 determines the output (I_{ea}) using the error (e) and the derivative of the error ($\dot{e}$). Further, the scaling factors C_d and C_e as determined using (8) and (11) are used to normalize the e and $\dot{e}$ for further utilization by the Fuzzy logic controller in the range [-1,1]. A scaling factor C_0 and C_1 as determined using (9) and (10) is also used to map the Fuzzy logic controller output and the Fuzzy-PID controller output respectively.

$$C_{d=}\min\left(T,\frac{L}{2}\right)\times C_e \tag{8}$$

$$C_0=\frac{1}{C\times C_e\left(\tau_c+\frac{L}{2}\right)} \tag{9}$$

$$C_1=max\left(T,\frac{L}{2}\right)\times C_0 \tag{10}$$

The input scaling factor C_e is:

$$C_e\equiv\frac{1}{r(t_r)-y(t_r)} \tag{11}$$

Where, τ_c is the closed-loop time constant and $r(t_r)$ and $y(t_r)$ are the reference and system output values at time $t=t_r$. These values correspond to the nominal operating point of the system.

IV. PERFORMANCE ANALYSIS OF THE BALANCING SCHEME

Simulation studies are conducted in MATLAB-Simscape to assess the performance of the proposed balancing scheme. The proposed balancing scheme and the Fuzzy-PID control algorithm are developed using MATLAB "Power Electronics Toolbox" and "Fuzzy Logic Toolbox" respectively. Then, the balancing performance is tested at different combinations of initial SOC of each cell in both the charging and discharging period. For visualization and analysis purposes SOC, voltage, and current of each cell are logged using a data acquisition unit throughout the charging and discharging cycle. The plots of SOC, voltage, and current of each cell during the charging and discharging period are shown in Fig. 9 and Fig. 10 respectively. The initial (at the beginning of balancing) and final SOC (at the end of balancing) of each cell during the charging and discharging period are summarized in Table II. To further demonstrate the superiority of the Fuzzy-PID-based method over the conventional mean SOC-based method, a comparative study is also conducted under the same initial condition.

A. *Balancing During Charging Period*

The plots of cell SOC, voltage, and current during the CCCV charging period are shown in Fig 9. It can be inferred from the SOC (Fig. 9(a)) and voltage (Fig. 9(b)) plot that the charging process is started with different initial points of SOC and voltage, however with the progress of the charging the SOC and voltage of individual cell are slowly approaching to each other. Near about 1310 seconds cell SOCs are converged, and the maximum difference is reduced below the threshold value ($\Delta SOC = 1\%$). It indicates the termination of the C2P balancing operation which is also confirmed by the current plot (Fig. 9(c) as there is no balancing current in the circuit after t=1310 seconds. Only a constant charging current of 4 A is drawn by the battery pack. The balancing results are shown in Table II. A maximum SOC difference of about 20% has been reduced to 1% within a very short period confirming the effectiveness of the proposed charge equalization scheme.

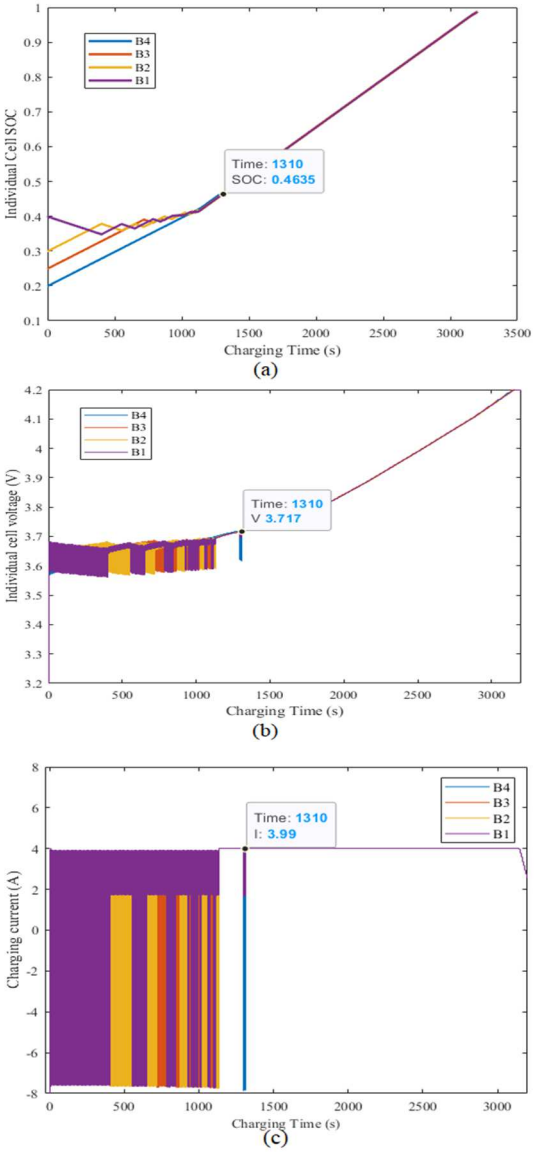

Fig. 9. The plot of (a) SOC, (b) cell voltage (c) current during simultaneous charging and balancing.

B. *Balancing During Discharging Period*

Similarly, during the discharging period, it can be evidenced from Fig. 10(c) that the balancing operation with the initial condition stated in Table II, stopped at about 1072 seconds as there is no stress of balancing current after that timestamp. Only a constant discharging current is drawn from the battery pack by the load. A similar conclusion can be made from the SOC (Fig.10(a)) and voltage plot (Fig.10(b)) of each cell during discharging period. With this result, it can be stated that the proposed balancing scheme is highly effective not only in the charging period but also in discharging period.

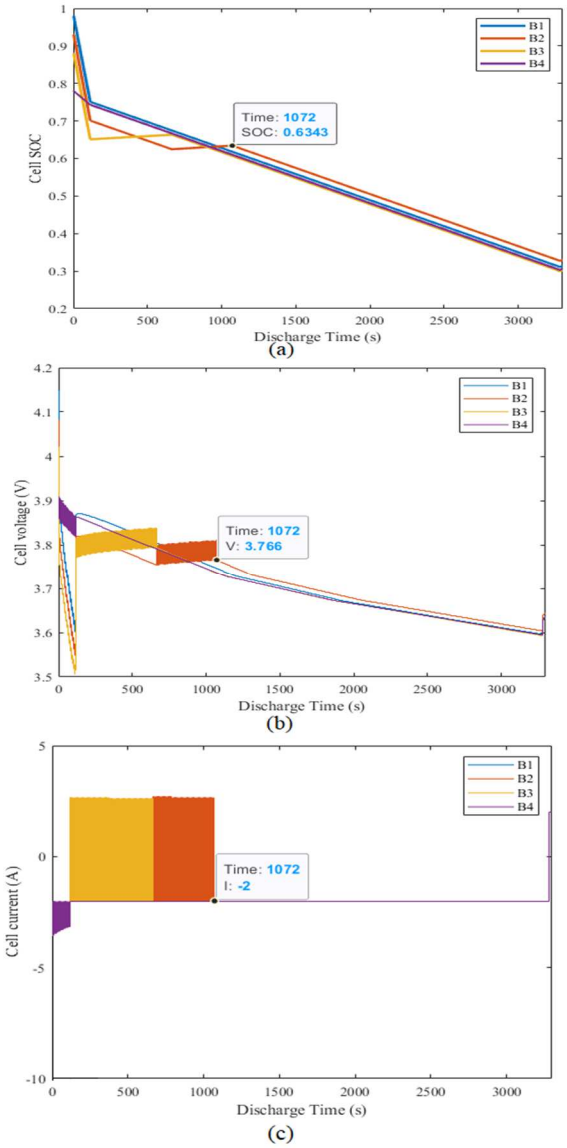

Fig. 10. The plot of (a) SOC, (b) cell voltage (c) current during simultaneous discharging and balancing.

TABLE II. TABLE INITIAL AND FINAL SOC OF EACH CELL

% SOC	Charging Period		Discharging Period	
	Initial	*Final (t=1310 s)*	*Initial*	*Final (t=1072 s)*
B1	40%	46.3%	98%	63.1%
B2	30%	46.5%	93%	63.4%
B3	25%	45.5%	88%	62.5%
B4	20%	46.5%	78%	62.5%
ΔSOC (Max)	20%	1%	20%	1%

C. Comparison with the state-of-the-art

Finally, to assess the superiority of the proposed algorithm compared to the traditional average SOC-based algorithm, a comparative study is conducted concerning the balancing time. The SOC plot during the charging period when the average SOC-based control algorithm is used is shown in Fig. 11. It is evidenced that a balancing time of 1590 seconds is required when the average SOC-based algorithm is used whereas with the same initial condition only about 1310 seconds (Fig. 9(a).) is required in case of the proposed algorithm.

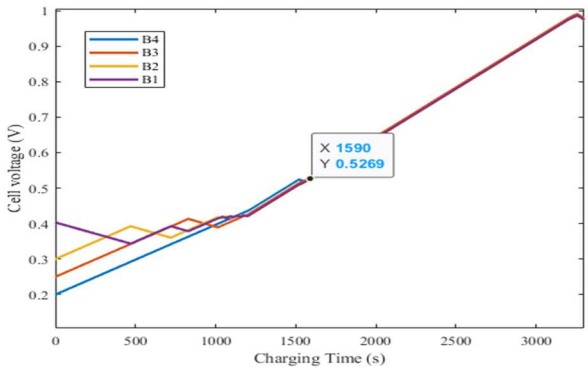

Fig. 11. The plot of cell SOC when the average SOC-based control algorithm is used during the charging period

V. CONCLUSION

This paper presents a non-dissipative (active) bidirectional DC-DC converter-based C2P2C charge balancing scheme for LIB pack with an advanced Fuzzy-PID controller. The supercapacitor is used as a temporary energy tank while shuttling the balancing energy to improve the speed and efficiency of cell balancing. It will also enhance the cycle life and reliability of the balancing circuitry. A simulation study conducted in MATLAB-Simscape indicated that the two-stage bidirectional charge equalization circuit is highly effective in charge balancing simultaneously during both the charging and discharging period. The fuzzy-PID-based control algorithm reduced the requirement of highly accurate SOC estimation in real-time which is very challenging and computationally expensive. The simulation results indicated that the proposed method is capable to reduce a 20% imbalance in only 1310 seconds and 1072 seconds during the charging and discharging period respectively. The comparative analysis demonstrated the proposed Fuzzy-PID-based control algorithm is more effective in comparison with the conventional average SOC-based control algorithm in terms of balancing speed. It is noticed that when the Fuzzy-PID control algorithm is used with the same balancing topology, the balancing time is reduced by around 280 seconds. The proposed scheme will help to develop more advanced but cost effective industry ready BMS.

REFERENCES

[1] X. Yang, L. Xi, Z. Gao, Y. Li, and J. Wen, "Analysis and Design of a Voltage Equalizer Based on Boost Full-Bridge Inverter and Symmetrical Voltage Multiplier for Series-Connected Batteries," *IEEE Trans. Veh. Technol.*, 2020, doi: 10.1109/TVT.2020.2974530.

[2] C. S. Lim, K. J. Lee, N. J. Ku, D. S. Hyun, and R. Y. Kim, "A modularized equalization method based on magnetizing energy for a series-connected lithium-ion battery string," *IEEE Trans. Power Electron.*, 2014, doi: 10.1109/TPEL.2013.2270000.

[3] K. M. Lee, Y. C. Chung, C. H. Sung, and B. Kang, "Active cell balancing of Li-Ion batteries using LC series resonant circuit," *IEEE Trans. Ind. Electron.*, vol. 62, no. 9, pp. 5491–5501, 2015, doi: 10.1109/TIE.2015.2408573.

[4] N. Nguyen, S. K. Oruganti, K. Na, and F. Bien, "An adaptive backward control battery equalization system for serially connected lithium-ion battery packs," *IEEE Trans. Veh. Technol.*, 2014, doi: 10.1109/TVT.2014.2304453.

[5] Y. Shang, Q. Zhang, N. Cui, B. Duan, and C. Zhang, "An optimized mesh-structured switched-capacitor equalizer for lithium-ion battery strings," *IEEE Trans. Transp. Electrif.*, 2019, doi: 10.1109/TTE.2018.2870971.

[6] Y. Shang, Q. Zhang, N. Cui, B. Duan, Z. Zhou, and C. Zhang, "Multicell-To-Multicell Equalizers Based on Matrix and Half-Bridge LC Converters for Series-Connected Battery Strings," *IEEE J. Emerg. Sel. Top. Power Electron.*, 2020, doi: 10.1109/JESTPE.2019.2893167.

[7] A. Samanta and S. Chowdhuri, "Active Cell Balancing of Lithium-ion Battery Pack Using Dual DC-DC Converter and Auxiliary Lead-acid Battery," *J. Energy Storage*, vol. 33, no. September, p. 102109, Jan. 2021, doi: 10.1016/j.est.2020.102109.

[8] A. Sani, C. K. Hu, Y. C. Hsieh, H. J. Chiu, and J. Y. Lin, "Switched-capacitor charge equalization circuit for series-connected batteries," *2016 IEEE 2nd Annu. South. Power Electron. Conf. SPEC 2016*, pp. 2–6, 2016, doi: 10.1109/SPEC.2016.7846016.

[9] K. Friansa, I. N. Haq, E. Leksono, N. Tapran, D. Kurniadi, and B. Yuliarto, "Battery module performance improvement using active cell balancing system based on Switched-Capacitor Boost Converter (S-CBC)," *Proceeding - 4th Int. Conf. Electr. Veh. Technol. ICEVT 2017*, vol. 2018-Janua, pp. 93–99, 2018, doi: 10.1109/ICEVT.2017.8323541.

[10] F. Baronti, G. Fantechi, R. Roncella, and R. Saletti, "High-efficiency digitally controlled charge equalizer for series-connected cells based on switching converter and super-capacitor," *IEEE Trans. Ind. Informatics*, vol. 9, no. 2, pp. 1139–1147, 2013, doi: 10.1109/TII.2012.2223479.

[11] B. Jiang, Y. Liu, X. Huang, and R. R. R. Prakash, "A New Battery Active Balancing Method with Supercapacitor Considering Regeneration Process," *IECON Proc. (Industrial Electron. Conf.*, vol. 2020-Octob, pp. 2364–2369, 2020, doi: 10.1109/IECON43393.2020.9254839.

[12] K. S. Tang, K. F. Man, G. Chen, and S. Kwong, "An optimal fuzzy PID controller," *IEEE Trans. Ind. Electron.*, 2001, doi: 10.1109/41.937407.

[13] S. Ban, J. Zhang, L. Zhang, K. Tsay, D. Song, and X. Zou, "Charging and discharging electrochemical supercapacitors in the presence of both parallel leakage process and electrochemical decomposition of solvent," *Electrochim. Acta*, 2013, doi: 10.1016/j.electacta.2012.12.056.

[14] J. M. Mendel, *Uncertain Rule-Based Fuzzy Systems: Introduction and New Directions*. 2017.

[15] A. Samanta and S. S. Williamson, "A Comprehensive Review of Lithium-Ion Cell Temperature Estimation Techniques Applicable to Health-Conscious Fast Charging and Smart Battery Management Systems," *Energies*, vol. 14, no. 18, p. 5960, Sep. 2021, doi: 10.3390/en14185960.